Boundary conditions for an instationary contact line of a viscous drop spreading on a plate

EINDHOVEN UNIVERSITY OF TECHNOLOGY
Department of Mathematics and Computing Science

RANA 96–17
September 1996

Boundary conditions for an instationary contact line of a viscous drop spreading on a plate

by

S.L. de Snoo

Reports on Applied and Numerical Analysis
Department of Mathematics and Computing Science
Eindhoven University of Technology
P.O. Box 513
5600 MB Eindhoven
The Netherlands
ISSN: 0926–4507

Boundary conditions for an instationary contact line of a viscous drop spreading on a plate.

SL de Snoo

Abstract

The flow of a glass drop is studied on micro-meter scale. This flow is described by a quasi-stationary Stokes-flow with a free surface, governed by surface tension and the contact line forces. We investigate the effects of the boundary conditions in the contact line region on the time evolution of a spreading drop. From several modifications of the continuum model the most suitable boundary conditions near the instationary moving contact line are a linear slip on the fluid-solid surface and a force on the contact line in order to generate the contact angle.

Numerical results of a finite element model show that the slip-coefficient influences the contact line velocity and that the size of the elements near the contact line has to be of the order of the slip-length for an accurate solution. The use of smaller elements results in stiff differential equations, thus restricting the time step of explicit methods.

1 Introduction

In glass technology many problems arise, varying in character and scale. One of them is the morphology of the glass under pressure. The glass here is to be seen as a (Newtonian) fluid, a situation which holds if the temperature is large enough (usually between 600 and 1200°C) to provide for a suitably low viscosity. In the production of CRTs the moulding process involves two scales. One is the global form of the screen, tenths of centimeters large, and one the small dimples in the glass, needed to have sufficient roughness on the surface e.g. to prevent reflections and for letting the fluorencent coating stick on it in a controlled way. The problem of the morphology of such a small dimple which is of a micrometer dimension is simplified here to the evolution of a liquid drop on a solid plate. This motion is mainly governed by the forces in the region around the contact line. The contact line is the boundary of the free surface (of the drop) and the solid plate.

Fluid-solid contact lines have been studied since the end of last century. Moving contact lines have received a lot of attention since the late sixties. However, most studies have been focusing on stationary moving contact lines, while we are interested in instationary contact lines with special attention for the mathematical formulation, numerical (finite element) modelling and the influence of such a contact line on the motion of a viscous fluid. The contact angle at a fluid-solid-gas interface, the surface tension and the no-slip conditions are macro scale effects of interactions on molecular level. We remark that the surface and contact line of a fluid are not sharply defined on this molecular level. Therefore it is not very surprising that problems may arise when one tries to model the contact line with continuum mechanics where this contact line is exactly defined. As clearly explained in [6, 7, 9] the combination of a no-slip condition and a moving contact line results in a singular problem. A modification of the boundary conditions of the problem can remove this singularity.

This paper is built up as follows. In §2 we analyse the characteristics of the glass flow in a mould and the motion of the drop. Then in §3 we discuss the motion of the contact line. It turns out the we first have to remove a singularity which arises in the formulation. This then gives us suitable boundary conditions. In §4 we briefly discuss a finite element formulation and indicate

how the subsequent simulations are carried out. The simulation of the spreading of a 10 μm small drop of glass at constant temperature is discussed in §5. Special attention will be given to the influence of the size of the elements. Finally we give some conclusions and suggestions in §6.

2 Glass flow at micrometer scale

In this section we will give a model description of the glass flow at a micrometer scale during the moulding process and show that this flow has the same characteristics as the spreading on a solid surface of a glass drop with the same length scale. The latter motion is simple to describe and an analytical approximation can be found using the method of matched asymptotic expansions, see [13]. This analytical approximation can be used to verify and validate our numerical model.

The motion of glass at temperatures above 600°C can be described by the Navier-Stokes equation for incompressible Newtonian fluids,

$$Re\left(Sr\frac{\partial \bar{\mathbf{u}}}{\partial \bar{t}} + (\bar{\mathbf{u}}\cdot\nabla)\bar{\mathbf{u}} \right) = -\nabla\cdot\bar{\sigma} + \frac{Re}{Fr}\bar{g}\,. \tag{1}$$

Here $\bar{\mathbf{u}}$ is the dimension free velocity, $\bar{t}$ the dimension free time, $\bar{g}$ the dimension free gravity and

$$\bar{\sigma} = \left(\nabla\bar{\mathbf{u}} + \nabla\bar{\mathbf{u}}^T\right) - \bar{p}\mathbf{I}\,, \tag{2}$$

the dimension free stress tensor, with the dimension free pressure $\bar{p}$. *Re*, *Sr* and *Fr* are the *Reynolds*, *Froude* and *Strouhal* numbers respectively, which characterise the flow. These numbers are expressed in the characteristic parameters of the flow. Using a pressure p_c and a length l_c, characteristic for the manufacturing process, and a density ρ and a viscosity μ, characteristic for glass at a certain temperature, a characteristic velocity

$$u_c = \frac{p_c l_c}{\mu} \tag{3}$$

and a characteristic time scale

$$t_c = \frac{l_c}{u_c} = \frac{\mu}{p_c}\,, \tag{4}$$

result. Consequently, the dimension free numbers are

$$Re = \frac{\rho l_c u_c}{\mu} = \frac{\rho p_c l_c^2}{\mu^2}\,, \quad Fr = \frac{u_c^2}{g l_c} = \frac{p_c^2}{g\mu^2}\,, \quad Sr = \frac{t_c l_c}{u_c} = 1\,, \tag{5}$$

with g the gravitational acceleration.

A typical value for the pressure during the moulding process is 10^5 kg/m^2. The length scale of the surface variations of interest in is 10 μm. The density of glass is 2500 kg/m^3 cf. [24]. The viscosity of glass strongly depends on the temperature. At 600°C the viscosity is 10^{12} $kg\,s/m^2$. At 700, 800 and 900°C one finds 4.10^8, 4.10^6 and 2.10^5 $kg\,s/m^2$ respectively. The Reynolds number for such a flow varies from 10^{-26} to 10^{-13}, and the quotient *Re/Fr* is of about 10^{-11}. Inertial and gravitational effects can thus be neglected. The motion of the fluid can thus be described adequately by the stationary Stokes-equations for incompressible fluids

$$\nabla \cdot \bar{\sigma} = 0, \tag{6}$$

$$\nabla \cdot \bar{\mathbf{u}} = 0. \tag{7}$$

The surface tension provides for the boundary conditions on the free surface

$$\sigma \mathbf{n} = (\kappa\gamma - P_{ext})\mathbf{n}. \tag{8}$$

Here κ is the curvature of the surface, γ the surface tension and P_{ext} the external pressure. In dimension free quantities this reads

$$\bar{\sigma}\mathbf{n} = \left(\frac{1}{Ca}\bar{\kappa} - \bar{P}_{ext}\right)\mathbf{n}, \tag{9}$$

with

$$Ca := \frac{u_c \mu}{\gamma} = \frac{p_c l_c}{\gamma}, \tag{10}$$

the so called capillary number.

As remarked above we will consider the spreading of a small drop on a solid surface as being typical for the phenomenon we are interested in. Hence we take the size of the drop equal to the typical length scale of 10 μm. The pressure in a stationary drop equals

$$p = 2\frac{\gamma}{r}, \tag{11}$$

with r the radius of the drop. The surface tension of glass equals 0.3 N/m. The pressure in a drop with a diameter of 10 μm is about 10^5 N/m^2, as was the pressure in the mould.

A major point of interest in the study of the evolution of a viscous blob under surface tension is the range of time scales present in the problem. These time scales can be found from a dimension analysis. A non-dimensional formulation based on the characteristic length l_c, surface tension γ, and viscosity μ one can define a characteristic velocity

$$u_c = \frac{\gamma}{\mu} \tag{12}$$

and a characteristic time scale

$$t_c = \frac{l_c}{u_c} = l_c \frac{\mu}{\gamma}. \tag{13}$$

At first sight it may seem strange that the characteristic velocity does not depend on the characteristic length scale. To understand this a sinusoidal disturbance of the surface can be considered. The velocity of the surface will be proportional to the ratio of the magnitude and the wavelength of the sinus and thus be independent of the characteristic length. The length scale of the geometry does not influence the velocity. On the other hand the characteristic time is proportional to the characteristic length. As a consequence smaller geometries will evolve faster. Under the influence of surface tension, perturbations of the surface with a short wavelength will smooth out quickly. The long time scales in a geometry will thus be more or less proportional to the largest length scale and the short time to the smallest length scale, which is zero in the continuous case and equal to the length scale of discretisation in the discrete case. This wide range of time scales may result in a stiff problem, when solving the differential equations numerically.

3 The moving contact line

The place where fluid-solid and fluid-gas interfaces meet is called the contact line (which is a single point in an axisymmetric formulation). At this line the two interfaces form an angle, the contact angle (see figure 1). The influence of the contact angle on fluid flow with a free boundary was first analysed by West in 1912 [27]. For a moving capillary with diameter a, he found a pressure drop (p) between the gas in front of the meniscus and the liquid at a distance L behind the meniscus to be given by

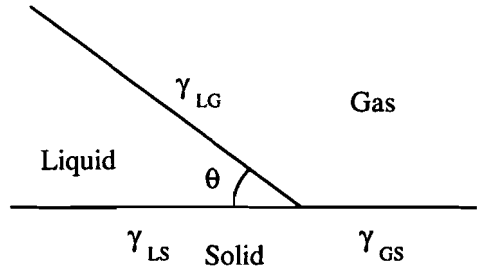

Figure 1: the contact angle θ.

$$p = 8\mu U\frac{L}{a^2} - 2\frac{\gamma}{a}\cos\theta\,, \tag{14}$$

with U the velocity of the contact line, μ the viscosity, γ the surface tension and θ the contact angle. In a stationary situation the velocity of the contact line is equal to the characteristic velocity u_c. Furthermore, if the distance L equals the diameter a, then

$$p = 8\frac{\gamma}{l_c}\left(Ca - \frac{\cos\theta}{4}\right). \tag{15}$$

This analysis shows that both the surface tension and the contact angle are relevant factors in a Stokes flow model if the capillary number is of the order of 1 or less.

3.1 The slip boundary condition

The modelling of a moving front of a Newtonian fluid with surface tension and a no-slip condition results in a singular problem at the contact line [6, 7, 9]. No-slip and a moving contact line are kinematically compatible, but give rise to a multi-valued velocity. The velocity at the contact line will be discontinuous, the stress tensor thus unbounded and unbounded forces are needed for the motion of the fluid at the contact line. There are two types of solutions to this singularity problem: the use of molecular dynamic modelling [16, 17, 25] and modification of the continuum mechanics model. The former is useful if one is interested in effects on molecular scale, but the latter is more practical for studying macro scale effects.

Several modifications to the continuum mechanics models can be made. The most common is the relaxation of the no-slip condition, which can be found in different forms resulting from different assumptions. One assumption is that the fluid is not fixed to the solid, but moves with a (non)-linear friction over the surface, the velocity thus being propotional to the shear [7, 8, 10, 12, 13, 14, 18, 19]. Such a slip is also observed in molecular dynamics simulations [17, 25]. One may also assume that the fluid is rolling over a rough surface [11]. The boundary condition resulting from this assumption is equivalent to the one obtained with friction. Another assumption for slip is that the fluid molecules need some time to get fixed to the solid [15]. This results in a region near the contact line where the fluid moves without friction. A weak point in this assumption is that the fluid in such a model is effectively not rolling over the surface, the contactline will always consist of the same material points [9]. For different models using slip, Dussan V. [8] has shown that the macro scale flow does not depend on the actual formulation of the slip. It depends only on the parameter defining the slip coefficient.

Slip models are not the only solution for the singularity problem. Another modification to the continuum mechanics model is the elimination of the contact line by assuming a precursor film

[2]. This film is a result of vapourization and diffusion of the fluid. The macro-scale flow obtained with this model is highly equivalent with the result of slip-models. However, Copley *et al.* [4] demonstrated that this assumption actually is not valid for glass, no precursor film is ever detected. A third modification would be to abandon the Newtonian character of the fluid. A shear thinning behaviour of the viscosity results in a bounded force, even though the velocity gradient is still unbounded [26]. Glass has such a shear thinning behaviour [23]. One of the problems encountered in this model is the increasing Reynolds number near the contact line. The flow is thus highly non-linear. The final modification is the introduction of a surface tension gradient as a result of molecular dynamics [22]. The fluid-gas and fluid-solid interfaces are both described by surface tensions. Chemical potentials and thermodynamic laws lead to the a parameter called the surface tension relaxation time, which characterizes the interval of time required for the formation of the interfacial structures. This model is very complicated for use in a numerical method.

All modifications of the continuum mechanics model have some unknown parameter and all models predict the same macro-scale flows. Boender *et al.* [3] have calculated the shape of the meniscus from a (known) angle of the surface at some distance from the solid while ignoring the region of a few *nm* from this point to the contact line. From these results it can be concluded that any model could be adequate for the description of the macro-scale flow. Knowing this and not being interested in the flow at *nm* scale, we allow ourselves to use a simple linear slip model, which of all modifications is the easiest to implement. This linear slip condition corresponds to a friction linear in the velocity of the fluid. The friction force has to be in balance with the tangential forces on the fluid surface, i.e.

$$(\sigma \mathbf{n}) \cdot \mathbf{t} = \beta \mathbf{u} \cdot \mathbf{t} = (\mu / \lambda) \mathbf{u} \cdot \mathbf{t}, \tag{16}$$

with σ the stress tensor, $\mathbf{t}$ and $\mathbf{n}$ the tangential and normal directions on the interface, β the slip coefficient and λ the slip length, which is usually between 1 and 100 *nm*. Since the fluid cannot move through the solid boundary we also have the boundary condition

$$\mathbf{u} \cdot \mathbf{n} = 0. \tag{17}$$

3.2 Dynamic contact angle

In literature there is no common agreement on how the contact angle at a moving contact line behaves. One of the problems is the fact that the dynamic contact angle is not well defined. Experimental and numerical investigations in the neighbourhood of the contact line show that the surface of the fluid surface undergoes rapid changes near the contact line up to *nm* scale [3, 20]. An interesting conclusion, given by Boender [3], is that the value of the contact angle (at 1 nm from the solid surface) is dominant when the velocity is low. The dynamic contact angle is then close to the static value, and the value of the contact angle is of little importance at higher velocities when viscous forces dominate. Considering this and the fact that we are mainly interested in the mathematical model for a micrometer-scale flow, we will base our model, like most researchers, on a contact angle equal to the static contact angle.

However, the prescription of a fixed contact angle is not an easy task. It requires the velocity of the free surface to be constant near the contact line. In stationary moving boundary flows this is not a problem, because the whole surface is moving with a constant velocity. Solutions for these problems can be found with iterative approximation of the surface shape, given the position of the contact line [1, 5, 19]. For an instationary contact line the position is a priori unknown and the velocity of the free surface is not constant. Therefore we will use another

approach to prescribe the contact angle, which has also been used by Bach and Hassager [1]: the precription of a force on the contact line.

The static contact angle can be expressed in terms of a force using Young's equation [28]

$$\gamma \cos\theta_S = \gamma_{GS} - \gamma_{LS} = F_S . \tag{18}$$

Here θ_s represents the static contact angle, γ_{GS} and γ_{LS} are the surface tension on the gas-solid and liquid-solid interface and F_S the resulting force on the contact line. We now assume that the force working at a moving contact line equals the force on a static contact line. Numerical results in § 5 will confirm that the contact angle obtained with this force and linear slip in fact equals the static contact angle. When using a finite element method, the force on the contact line results in a natural boundary condition, while a fixed contact angle would result in an essential boundary condition. The former are much easier to handle.

4 Finite Element Formulation

For the solution of the Stokes equation we use a finite element method based on the weak formulation:

$$\int_\Omega -\mu\left(\nabla\mathbf{u} + (\nabla\mathbf{u})^T\right) : \nabla\mathbf{v}\, d\Omega + \int_\Omega p\nabla\cdot\mathbf{v}\, d\Omega + \int_\Gamma \mathbf{f}\cdot\mathbf{v}\, d\Gamma = 0 , \tag{19}$$

$$\int_\Omega (\nabla\cdot\mathbf{u}) q\, d\Omega = 0 , \tag{20}$$

where **v** and q represent the test functions and **f** represents the natural boundary condition:

$$\mathbf{f} = \sigma\mathbf{n} , \tag{21}$$

which corresponds to a force on the surface of the fluid.

For the implementation of the surface tension we use a formulation described by Bach and Hassager [1]. Application of the Frenet formula

$$\frac{d\mathbf{t}}{ds} = \kappa\mathbf{n} \tag{22}$$

and partial integration of the weak formulation of the surface tension force results in the formulation

$$\begin{aligned}\int_{s_0}^{s_1} \mathbf{f}_\gamma \cdot \mathbf{v}\, ds &= \int_{s_0}^{s_1} (-P_{ext} + \kappa\gamma)\mathbf{n}\cdot\mathbf{v}\, ds \\ &= -\int_{s_0}^{s_1} P_{ext}\mathbf{n}\cdot\mathbf{v}\, ds - \gamma\int_{s_0}^{s_1} \mathbf{t}\cdot\frac{d\mathbf{v}}{ds} ds + \gamma[\mathbf{v}\cdot\mathbf{t}]_1 - \gamma[\mathbf{v}\cdot\mathbf{t}]_0 ,\end{aligned} \tag{23}$$

which can easily be implemented in a finite element model. The advantage of this formulation is that the surface does not have to be smooth ($S \in C^0$). Another advantage is that the last two terms on the right-hand side describe a force on the edges of a surface which can be used to implement the contact angle as mentioned above in section 3.2. The above formulations are given in general co-ordinates. The axisymmetric formulations can be found in the appendix.

For the discretization of the problem we use a Galerkin formulation and triangular Taylor-Hood elements with quadratic approximation of the velocity and a linear approximation of the pressure. This element satisfies the Babuška-Brezzi condition, is accurate and simple to implement. Moreover we do not want to use a penalty method, because the introduced artificial

compressibility might give unrealistic solutions due to the large variation in pressure near the contact line.

The problem defined above is a stationary one. The reduction to a stationary situation is allowed since the inertial effects can be neglected. Actually our problem is quasi-stationary, as the boundary is moving. For the time evolution of the drop we use the following equation for the displacement,

$$\dot{\mathbf{x}} = \mathbf{u}. \tag{24}$$

Here $\dot{\mathbf{x}}$ is the velocity of the boundary and $\mathbf{u}$ is the velocity of the fluid at the boundary. For the time integration in equation (24) an Euler-forward scheme is used. Every time step a completely new mesh is generated. The time required for this is acceptable compared to the time needed to build the matrix and solve the linear equations. It is less than 15% of the total time. The system of equations is solve by means of a LU-decomposition.

We have implemented the problem using the finite element package Sepran [21]. The mesh generation is done by an updated version of the mesh generator of this package which can handle large differences in element size without problems.

5 Numerical investigation of a model of an axisymmetric drop

We have chosen to simulate a drop similar to the one used by Hocking and Rivers [13] in their calculations and observations. This is a drop of glass with a radius $r_0 = 10^{-5}$ m. The temperature is kept constant at 800°C. The viscosity at this temperature $\mu = 10^5$ Ns/m^2. The surface tension $\gamma = 0.30$ N/m. The force on the contact line $F_{CL} = 0.295$ N/m corresponds to a stationary contact angle of 10°. We do not vary this contact angle like Hocking, because a variation in the contact angle of 5° gives a variation in the contact line force less than 2%. This would only give a significant variation in the solution near equilibrium, which would not be attained in our computations.

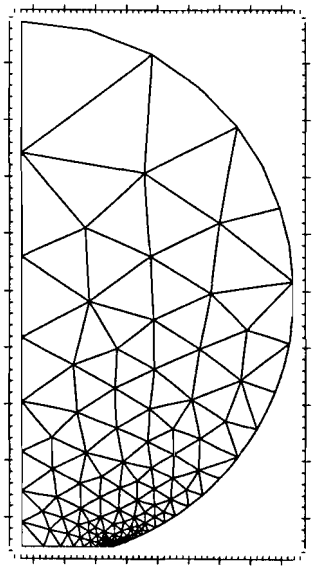

Figure 2:
mesh of the drop.

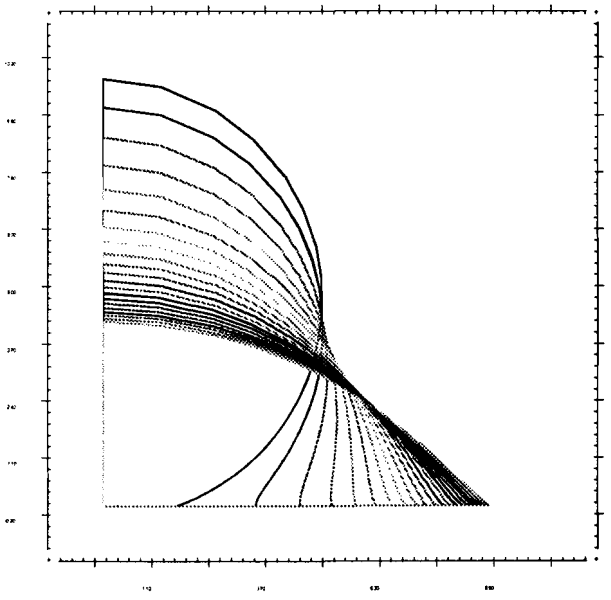

Figure 3: evolution of the drop in 10 time units.

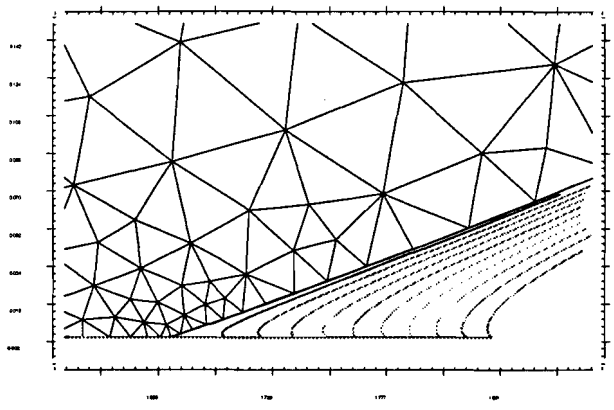

Figure 4: evolution of the surface near the contact line during 0.02 time units.

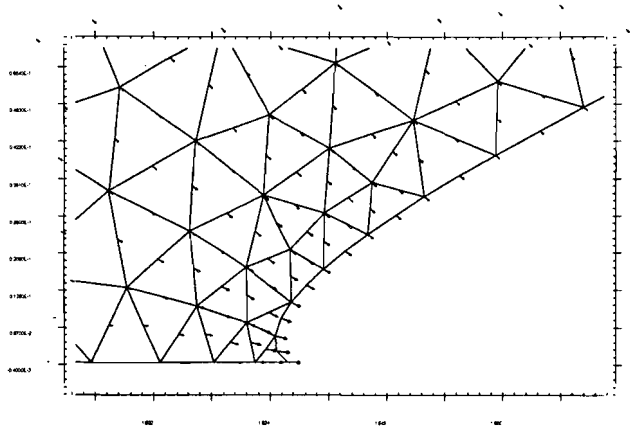

Figure 5: velocity field near the contact line.

Figure 2 shows the finite element mesh used in the computations. Figure 3 shows the evolution of the drop, with slip length $\lambda = 10^{-6}$ m, during 10 time units. A close-up of the contact line region during the first 0.02 time units is given in figure 4, from which it appears that in this region the shape of the surface does not vary much after a very short transitional period. This already shows that the evolution of the drop is a stiff problem, i.e. there is a time scale in the evolution, the initial contact line movement, which is much shorter than the time scale of interest, the evolution of the drop. As explained in section 2.2 this stiffness is introduced by the small elements on the surface.

The influence of the use of larger elements on the velocity of the contact line is shown in figure 6. The wiggles present in this figure are due to small variations in the size of the elements during the evolution of the geometry. They are not a result of an instability in the time integration (as we carefully checked). These results show that small elements are needed for an accurate solution of the evolution of the drop. This can be understood from looking at the velocity field (figure 5). The velocity is nearly constant in this region accept at the solid surface where the velocity decreases exponentially, with a characteristic length comparable with the slip length (figure 7). The use of elements larger then the slip length results in a poor approximation of the velocity. However, the error introduced in the velocity near the contact line results in an acceptable error for an element size up to 50 times the slip length. Larger element sizes give a significant error in the evolution of the drop.

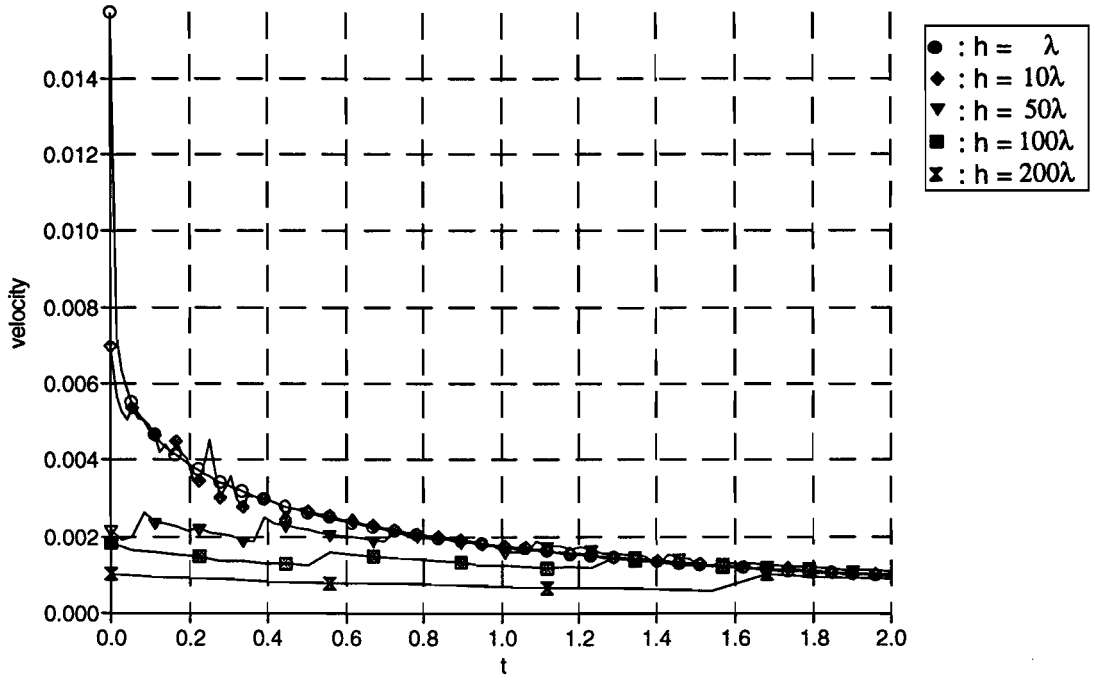

Figure 6: contact line velocity as a function of the element size on the contact line.

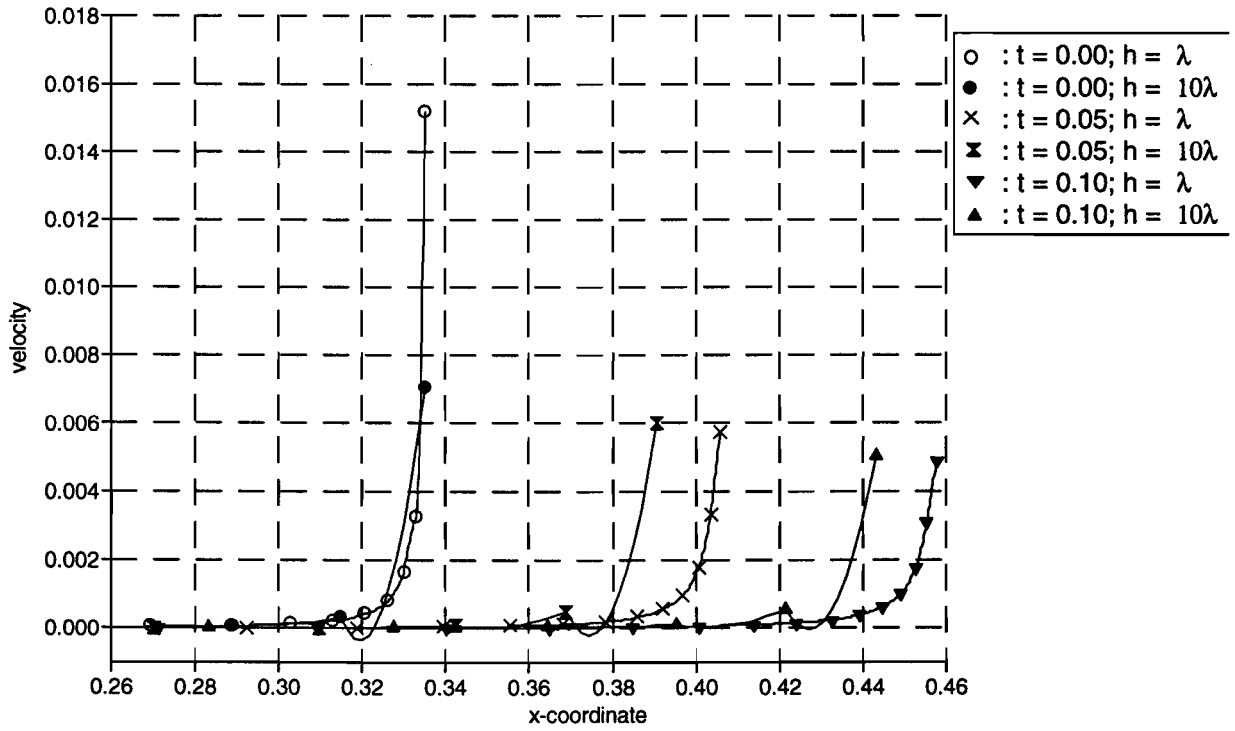

Figure 7: velocity of the fluid at the boundary with the solid.

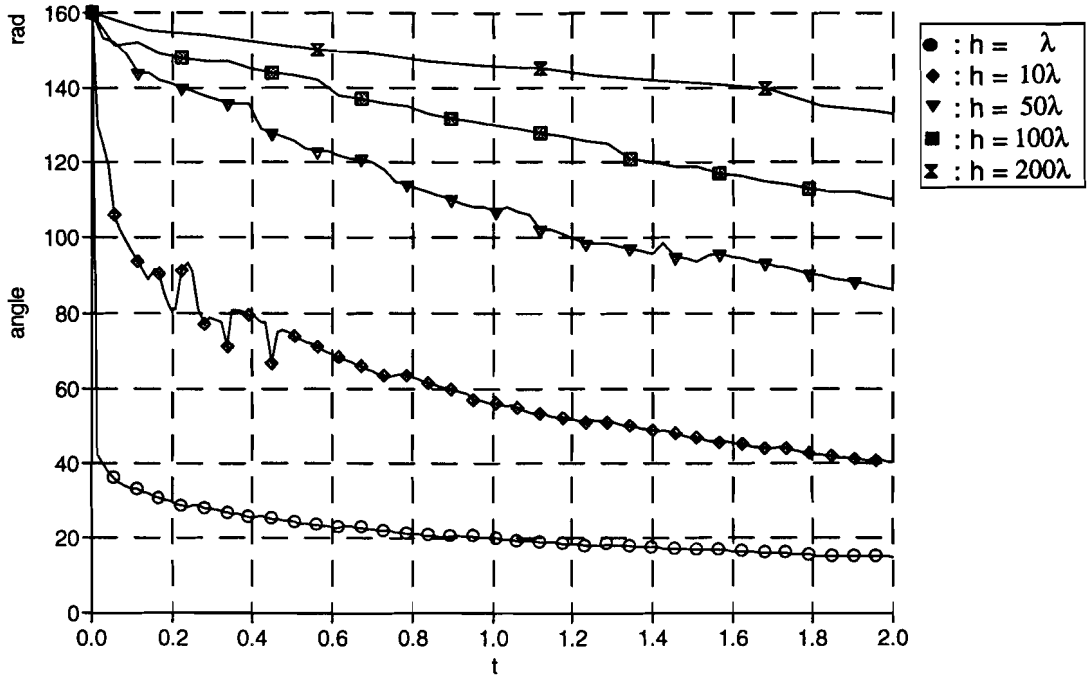

Figure 8: microscopic contact angle in the time for different element sizes.

The microscopic contact angle in the discretized case, the angle at the corner of the element at the contact line is shown in figure 8. One can see that for elements with a size equal to the slip length the microscopic contact angle corresponds to the static contact angle. For larger elements this is clearly not true, although the velocity is well approximated (figure 6).

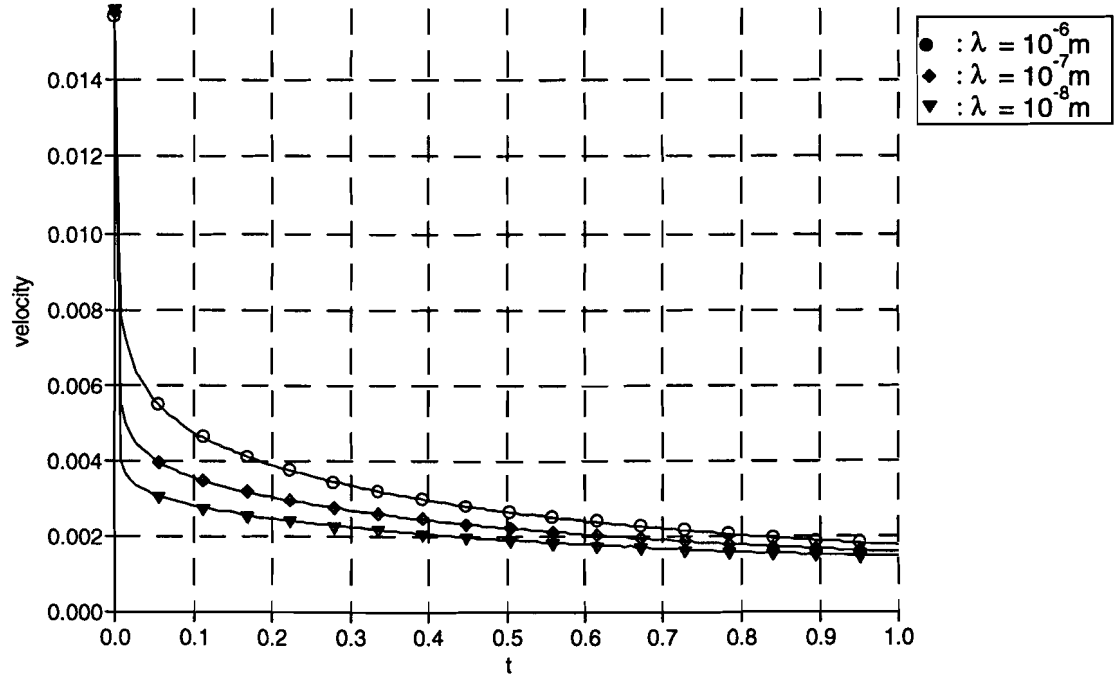

Figure 9: variation velocity as function of the slip length.

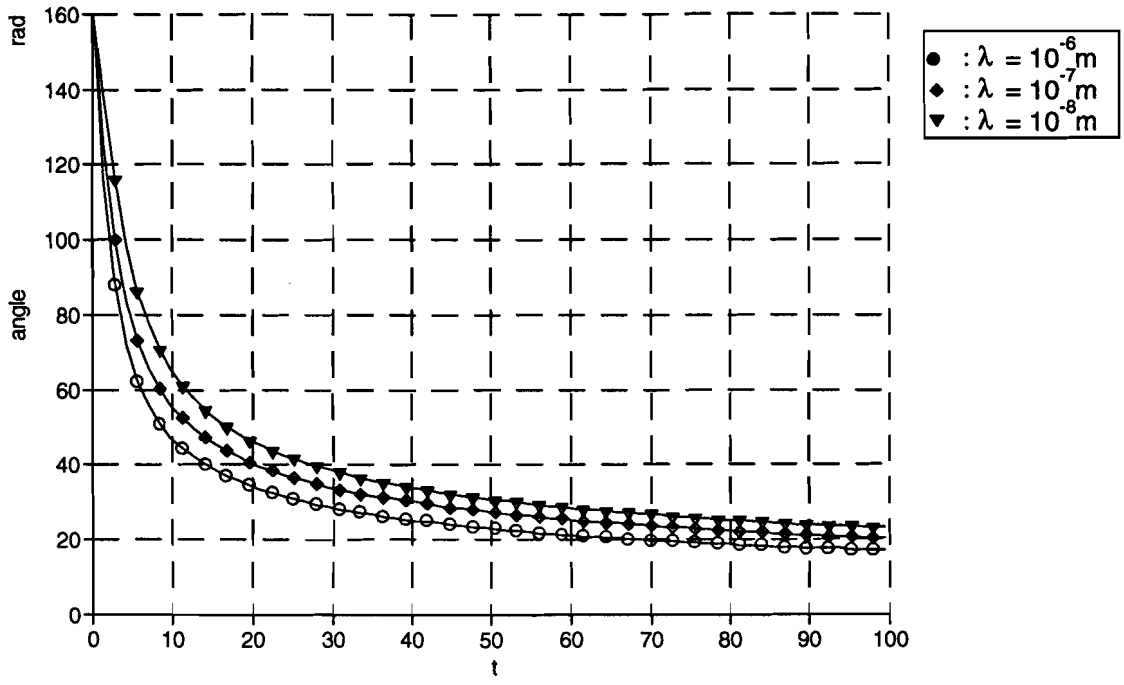

Figure 10: evolution of the angle of a spherical segment fitted on the drop for different slip lengths.

The velocity of the contact line also depends on the slip length as can be seen in figure 9. The slip length λ has been varied using values of 10^{-6}, 10^{-7} and 10^{-8} *m*. For a comparison of our results with the calculations of Hocking we can also compute the evolution of the shape of the drop as a function of the slip length, see figure 10. The shape is expressed in the angle between the surface and a spherical segment fitted on the drop. The correspondence of our results with those of Hocking and Rivers is remarkable.

6 Conclusions and Suggestions

As a first stage for the simulation of the moulding of glass we have investigated a model for the description of the motion of dynamic contact lines. The example of the spreading drop demonstrates that the instationary motion of a contact line can be modelled adequately, assuming linear slip on the solid-fluid boundary and a force on the contact line. The results obtained with our finite element model correspond to the results obtained by Hocking and Rivers [13].

The velocity of the contact line and thus the evolution of the drop, depends on the slip length, a parameter which is not exactly known for glass. Unfortunately, near the contact line quite small elements are needed for an accurate solution. Elements larger than 50 times the slip length result in significant errors in the velocity of the contact line. This is due to the exponential decay of the velocity near the contact line. However, this element size is much larger than the elements used by Lowndes [19], who needed a size of 0.1 of the slip-length. This difference is due to the use of a force on the contact line instead of the prescription of the contact angle.

Small compared with scale of drop..

The fact that the elements near the contact line are much smaller than the drop introduces stiffness in the numerical time integration, thus restricting the timestep of explicit methods.

Computational efforts can be reduced significantly by using implicit time integration methods. An alternative formulation of the contact line flow by means of some special large element at the contact line might also solve this problem.

For a full description of the flow of glass during a moulding process, the model described in this article has to be extended. The external pressure and the geometry of the mould have to be included. The temperature dependence of the viscosity has to be added too. For this the thermal energy equation, including radiative heat transfer, has to be added.

Acknowledgement

The authors wish to acknowledge useful discussions on the subject with Prof. G de With.

References

[1] Bach P and Hassanger O: An algorithm for the use of the Lagrangian specification in Newtonian fluid mechanics and applications to free-surface flow, J Fluid Mech. 1985, vol 152, 173-190

[2] Bascom WD, Cotting RL and Singleterry CR: Dynamic surface fenomena in the spontaneous spreading of oils on solids, In 'Contact Angles, Wettability and Adhesion' (RE Gould) p 355 Washington DC: Am Chem Soc.

[3] Boender W, Chesters AK and Van der Zanden AJJ: An approximate solution of the hydrodynamic problem associated with an advancing liquid-gas contact line, Int. J. Multiphase Flow, vol 17, 661-676, 1991

[4] Copley GJ, Rivers AD and Smith R: Reappraisal of contact angle measurements of sodium and potassium silicate glasses on platinum in air, Glass Technology Vol 13 No 2 April 72, 50-53

[5] Cuvelier C: Some numerical methods for the solution of capillary free boundaries governed by the Navier-Stokes equations, reports of the faculty of mathematics and informatics 8769, technical university Delft, 1987

[6] Davis SH: Contact-line problems in fluid mechanics, J of Applied Mechanics, dec 1983, vol 50, 977-982

[7] Dussan V. EB and Davis SH: On the motion of a fluid-fluid interface along a solid surface, J Fluid Mech. 1974, vol 65, 71-95

[8] Dussan V. EB: The moving contact line: slip boundary condition, J FLuid Mech 1976, vol 77 665-684.

[9] Dussan V. EB: On the spreading of liquids on solid surfaces: static and dynamic contact angles, Ann. Rev. Fluid Mech. 1979, 11:371-400

[10] Ford ML and Nadim A: Thermocapillary migration of an attachted drop on a solid surface, Phys Fluids 6, september 1994, 3183-3185

[11] Hocking LM: A moving liquid on a rough surface, J Fluid Mech 1976, vol 76, 801-817

[12] Hocking LM: A moving fluid interface. Part 2. The removal of the force singularity by a slip flow, J Fluid Mech 1977, vol 79, 209-229

[13] Hocking LM and Rivers AD: The spreading of a drop by capillary action, J Fluid Mech 1982, vol 121, 425-442

[14] Hocking LM: The spreading of drops with intermolecular forces, Phys. Fluids 6, 10 october 1994

[15] Huh C and Mason SG: The steady movement of a liquid meniscus in a capillary tube, J Fluid Mech 1971, vol 81, 401-419.

[16] Koplik J, Banavar JR and Willemsen JF: Molecular dynamics of Poiseuille flow and moving contact lines, Phys Rev Letters, 1988, vol 60, 1282-1285

[17] Koplik J, Banavar JR and Willemsen JF: Molecular dynamics of fluid flow at solid surfaces, Phys. Fluids A 1(5) May 1989, 781-794

[18] Lacey AA: The motion with slip of a thin viscous droplet over a solid surface, Studies in applied mathematics, 67:217-230, 1982.

[19] Lowndes J: The numerical simulation of the steady movemnet of a fluid meniscus in a capillary tube, J. Fluid Mech 1980 vol 101 p 631-646

[20] Ngan CF and Dussan V. EB: On the nature of the dynamic contact angle: an experimental study, J Fluid Mech, 1982 vol118, p 27-40

[21] Sepran, Finite Element Toolbox, Ingenieursbureau Sepra, Leidschendam (Netherlands), 1993

[22] Shikhmurzaev YD: The moving contact line on a smooth solid surface, Int. J. Multiphase Flow, vol 19, pp 589-610, 1993.

[23] Simmons JH and Simmons CJ: Nonlinear visous flow in glass forming, Ceramic Bulletin, vol 68 no 11, 1989.

[24] Simonis F, NCNG-Glass course, Handbook for the Dutch Glass Production (in Dutch), TNO-TPD Glass Technology

[25] Thompson PA and Robbins MO: Simulations of contact line motion: slip and dynamic contact angle, Phys Rev Letters, august 1989, vol 63, 766-769

[26] Weidner DE and Schwartz LW: Contact-line motion of shear-thinning liquids, Phys. Fluids 6 (11) Nov 94, 3535-3538

[27] West GD: On the resistance to the motion of a thread of mercury in a glass tube, Proc. Roy. Soc. A 86, 20, 1911-1912.

[28] Young T: An essay on the cohesion of fluids, Philos. Trans. R. Soc. London 95:65-87, 1805

Appendix: Axisymmetric formulation

The axisymmetric formulation for a Stokes flow with surface tension is not as simple as one might hope. Some unexpected terms arise in the weak formulation of the Stokes equation,

$$\int_\Omega -\mu\left(\nabla\mathbf{u}+(\nabla\mathbf{u})^T\right):\nabla\mathbf{v}\,d\Omega+\int_\Omega p\nabla\cdot\mathbf{v}\,d\Omega-\int_\Gamma \mathbf{f}\cdot\mathbf{v}\,d\Gamma=0\,, \tag{A.1}$$

and the surface tension boundary condition

$$\sigma\mathbf{n}=\left(-p_{ext}+\gamma\kappa\right)\mathbf{n}\,. \tag{A.2}$$

For the evaluation of the first term in (A.1) we need the gradient of **u** in cylindrical coordinates,

$$\nabla\mathbf{u}=\begin{pmatrix} u_{r,r} & u_{\varphi,r} & u_{z,r} \\ \dfrac{u_{r,\varphi}-u_\varphi}{r} & \dfrac{u_{\varphi,\varphi}+u_r}{r} & \dfrac{u_{z,\varphi}}{r} \\ u_{r,z} & u_{\varphi,z} & u_{z,z} \end{pmatrix}. \tag{A.3}$$

Here $u_{r,r}$ denotes the r-derivative of the r component of **u**. This gradient is substituted in the double inproduct of stress tensor and test function **v**, yielding

$$\begin{aligned}\left(\nabla\mathbf{u}+\nabla\mathbf{u}^T\right):\nabla\mathbf{v}=&\begin{pmatrix} 2u_{r,r} & u_{\varphi,r}+\dfrac{u_{r,\varphi}-u_\varphi}{r} & u_{z,r}+u_{r,z} \\ u_{\varphi,r}+\dfrac{u_{r,\varphi}-u_\varphi}{r} & 2\left(\dfrac{u_{\varphi,\varphi}+u_r}{r}\right) & \dfrac{u_{z,\varphi}}{r}+u_{\varphi,z} \\ u_{z,r}+u_{r,z} & \dfrac{u_{z,\varphi}}{r}+u_{\varphi,z} & 2u_{z,z} \end{pmatrix}:\begin{pmatrix} v_{r,r} & v_{\varphi,r} & v_{z,r} \\ \dfrac{v_{r,\varphi}-v_\varphi}{r} & \dfrac{v_{\varphi,\varphi}+v_r}{r} & \dfrac{v_{z,\varphi}}{r} \\ v_{r,z} & v_{\varphi,z} & v_{z,z} \end{pmatrix} \\ =&\,2u_{r,r}v_{r,r}+\left(u_{\varphi,r}+\frac{u_{r,\varphi}-u_\varphi}{r}\right)\left(\frac{v_{r,\varphi}-v_\varphi}{r}\right)+\left(u_{z,r}+u_{r,z}\right)v_{z,r}+ \\ &\left(u_{\varphi,r}+\frac{u_{r,\varphi}-u_\varphi}{r}\right)v_{\varphi,r}+2\left(\frac{u_{\varphi,\varphi}+u_r}{r}\right)\left(\frac{v_{\varphi,\varphi}+v_r}{r}\right)+\left(\frac{u_{z,\varphi}}{r}+u_{\varphi,z}\right)v_{\varphi,z}+ \\ &\left(u_{z,r}+u_{r,z}\right)v_{z,r}+\left(\frac{u_{z,\varphi}}{r}+u_{\varphi,z}\right)\frac{v_{z,\varphi}}{r}+2u_{z,z}v_{z,z}\end{aligned} \tag{A.4}$$

In the axisymmetric case there is no dependence on φ, so all terms with φ vanish and equation (4) is reduced to

$$\left(\nabla\mathbf{u}+\nabla\mathbf{u}^T\right):\nabla\mathbf{v}=\left(2u_{r,r}v_{r,r}+2\frac{u_rv_r}{r^2}+u_{r,z}v_{r,z}\right)+\left(u_{z,r}v_{r,z}\right)+\left(u_{r,z}v_{z,r}\right)+\left(u_{z,r}v_{z,r}+2u_{z,z}v_{z,z}\right) \tag{A.5}$$

The divergence of **v**, present in the pressure term of (1), equals

$$\nabla\cdot\mathbf{v}=\frac{(rv_r)_{,r}}{r}+\frac{v_{\varphi,\varphi}}{r}+v_{z,z}\,. \tag{A.6}$$

In axisymmetric coordinates the second term on the right hand side vanishes.

The third term in equation (1) corresponds to the boundary conditions. The boundary condition for the free surface, the surface tension

$$\sigma\mathbf{n} = \left(-p_{ext} + \gamma\kappa\right)\mathbf{n}, \tag{A.7}$$

is more complicated. The mean curvature of the surface κ, is the sum of the two principal curvatures,

$$\kappa_1 = \frac{1}{R_1} \text{ and } \kappa_2 = \frac{1}{R_2} \tag{A.8}$$

RR

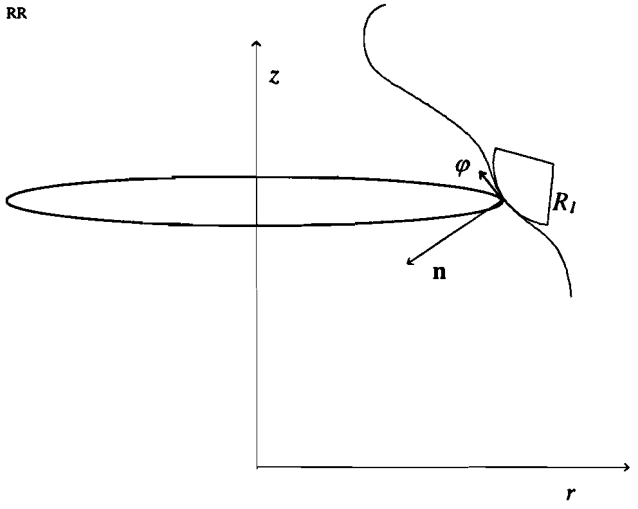

Figure A.1:curvature in the r-z plane.

In an axisymmetric case one curvature is the curvature in the r-z plane (see figure A.1.).

$$\kappa_1\mathbf{n} = \mathbf{t}_{,s}. \tag{A.9}$$

The other curvature is the curvature in the plane constructed by the normal of the surface and a line perpendicular to the normal and the r-z plane (the φ-direction),

$$\kappa_2 = \mathbf{t}_{\varphi,\Gamma}\mathbf{n} = -\frac{n_r}{r}. \tag{A.10}$$

The derivative of t along the boundary cannot be computed for a boundary which is not smooth. This derivative can be eliminated by means of partial integration

$$\begin{aligned}\int_\Gamma \gamma\kappa_1\mathbf{n}\cdot\mathbf{v}\,d\Gamma &= \int_s\int_\varphi \gamma\mathbf{t}_{,s}\cdot\mathbf{v}r\,d\varphi\,ds = 2\pi\int_s \gamma\mathbf{t}_{,s}\cdot\mathbf{v}r\,ds \\ &= 2\pi\left(\gamma\mathbf{t}\cdot\mathbf{v}r\right)\Big|_0^1 - 2\pi\int_s \gamma\mathbf{t}\cdot\left(\mathbf{v}r\right)_{,s}\,ds \\ &= 2\pi\left(\gamma\mathbf{t}\cdot\mathbf{v}r\right)\Big|_0^1 - 2\pi\int_s \gamma\mathbf{t}\cdot\left(\mathbf{v}_{,s}r + \mathbf{v}r_{,s}\right)ds\end{aligned} \tag{A.11}$$

This equation can be evaluated for a piece-wise smooth boundary. The assembled equation for the surface tension finally reads

$$\int_\Gamma \left(-p_{ext} + \gamma\kappa\right)\mathbf{n}\cdot\mathbf{v}\,d\Gamma = -2\pi\left[\int_s \left(p_{ext}r + \gamma n_r\right)\mathbf{n}\cdot\mathbf{v}\,ds - \int_s \gamma\mathbf{t}\cdot\left(\mathbf{v}_{,s}r + \mathbf{v}r_{,s}\right)ds + \left(\gamma\mathbf{t}\cdot\mathbf{v}r\right)\Big|_0^1\right] \tag{A.12}$$

PREVIOUS PUBLICATIONS IN THIS SERIES:

Number	Author(s)	Title	Month
96–09	H.J.C. Huijberts	Combined partial feedback and input-output linearization by static state feedback for nonlinear control systems	May '96
96–10	A.F.M. ter Elst D.W. Robinson	Analytic elements of Lie groups	May '96
96–11	S.L. de Snoo R.M.M. Mattheij G.A.L. van de Vorst	Modelling of glass moulding, in particular small scale surface changes	July '96
96–12	S.J.L. van Eijndhoven	Hilding's theorem for Banach spaces	August '96
96–13	A.F.M. ter Elst D.W. Robinson	Second-order subelliptic operators on Lie groups I: complex uniformly continuous principal coefficients	August '96
96–14	A.F.M. ter Elst D.W. Robinson	High order divergence-form elliptic operators on Lie groups	August '96
96–15	A.F.M. ter Elst D.W. Robinson	Second-order subelliptic operators on Lie groups II: real measurable principal coefficients	August '96
96–16	A.F.M. ter Elst D.W. Robinson	Second-order strongly elliptic operators on Lie groups with Hölder continuous coefficients	August '96
96–17	S.L. de Snoo	Boundary conditions for an instationary contact line of a viscous drop spreading on a plate	September '96